Nematic liquid crystal spatial light modulator's response to total-dose irradiation

Stephen DeWalt, Kyle Miller, Ball Aerospace & Technologies Corp.
Jay Stockley, Boulder Nonlinear Systems, Inc.

Abstract

Liquid crystal spatial light modulators are emerging as a potential replacement to traditional optical beam steering methods. The performance of these devices for optical communication systems in the radiation environment for geostationary orbits (GEO) are of interest for applications in the next generation of satellites. As an initial investigation to the study presented, several liquid crystals were irradiated to total dose levels consistent with expected GEO environments. Parameters of retardation, contrast ratio and primary power current were monitored at incremental stages during the test and are presented.

1. Introduction

This work was performed under the U.S. Air Force Research Laboratory/VSSV, SBIR Phase 1 contract F29601-03-M-0114. The results of total ionizing dose measurements on samples of Boulder Nonlinear Systems' (BNS) Liquid Crystal (LC) devices and an LC integrated onto a complementary metal-oxide semiconductor (CMOS) circuit chip to form a spatial light modulator (SLM) or optical phased array (OPA) are detailed. The tests were designed to evaluate critical SLM performance parameters. The primary goal of the testing is to determine the ability of an SLM to continue to function as a phase modulator after exposure to total ionizing doses typical of communication satellite systems.

Testing was performed in two parts. Part One consisted of the LC devices and Part Two consisted of a liquid crystal on silicon (LCoS) spatial light modulator. This two part testing was designed to distinguish the degradation between the LC and the SLM backplane.

For Part One testing, two device performance parameters were measured, retardation and contrast ratio. Neither parameter showed any significant degradation under the testing conditions up to a total ionizing dose of 200k rad(Si) to within measurement error. A total of twenty devices were used in Part One, of which sixteen were characterized and irradiated with the remaining four devices used as experimental controls. Of the twenty devices, ten were intrinsically optimized for a wavelength of light at 1.55 μm and ten devices for 2.0 μm wavelength. Both wavelength devices were irradiated first under unbiased and then biased conditions.

For Part Two testing, two SLM devices were tested. The performance parameters measured were input CMOS current and phase modulation depth. The first device, serial number BS145, was dosed up to 10k rad(Si) under biased conditions. Since no effects were seen, a second SLM was prepared and tested. The second SLM device, serial number BS223, gapped for optimum modulation at 1.55 μm wavelength light, was characterized, irradiated to a total ionizing dose of 208k rad(Si) and allowed to anneal, all under biased conditions. Unless otherwise stated all SLM results discussed below are for this second device.

Testing took place at the MRC-LL facility in Colorado Springs, CO. Testing generally conformed to MIL-STD-883, Method 1019.6

2. Part One Test Articles

The Part One devices were constructed of a standard liquid crystal material manufactured by EM Industries and used in the commercially available Spatial Light Modulators from BNS. The LC material is purchased as a commercial item without specific lot controls by BNS. The commercially available nematic LC material contained in all devices tested was BL087. The specifications of the material are included in Appendix B. This LC material was sandwiched between two optical flats to construct twenty test cells. The cells were built using spacers of two different thicknesses, which resulted in devices that act as phase modulators for optical wavelengths of 1.55 microns and 2 microns.

2.1 Test Article Description

The LC cells used in these tests consist of two fused silica flat glass substrates each having a transparent coating of Indium Tin Oxide (ITO) on one side and a broad band (0.8 μm - ~2 μm) MgF_2 coating on the opposite side, see Figure 2-1. A polyimide alignment layer is spun onto the ITO side of the substrates, baked and buffed with felt. The glass substrates are gapped using spherical glass spacers in ultra violet cured epoxy around the periphery. Once the cell thickness is fixed by curing the epoxy, the devices are filled with liquid crystal material using capillary action. Two different sets of spacers were used: 4.1 μm and 4.9 μm. These spacer gaps were chosen to represent phase modulators for 1.55 μm and 2 μm wavelengths, respectively. The overall dimensions of the LC cell test units are ~12 mm x 9 mm x 4 mm.

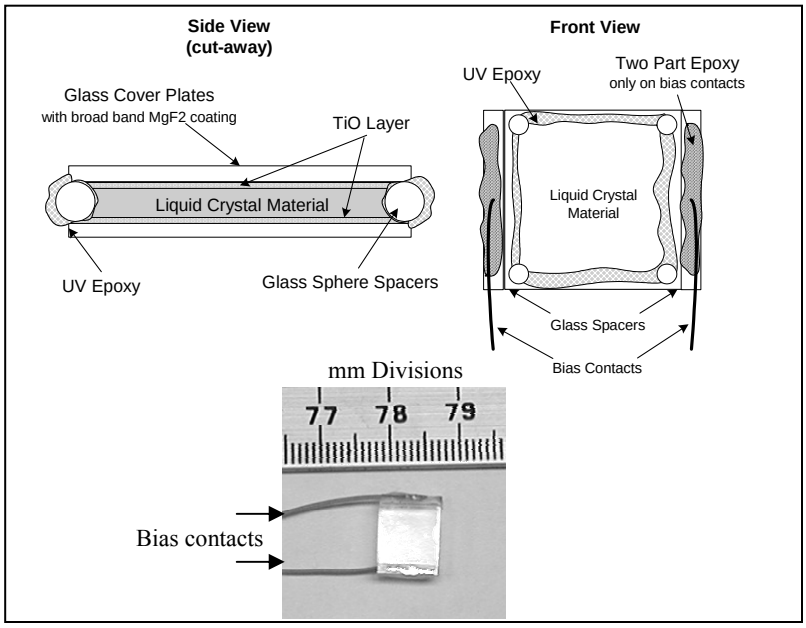

Figure 2-1. *Shown is the construction of the LC unit cell along with a photo of an LC device.*

The LC material mixture used in the test units is commercially available BL087 from EM Industries. Bias wires are soldered onto all the test units using indium wire then, for tension relief, two-part ultra-violet curing epoxy is used to secure the wires to the LC cell.

2.2 Operational Parameters

The two measurements performed on the LC cells were retardation and contrast ratio. While the end application (beam steering) requires phase-only modulation, the phase modulation depth can be determined from retardation.

Since the optic axis of the unbiased, or un-switched LC lies perpendicular to the surface of incident broadband light, see Figure 2-2, light is evenly split between the ordinary and extraordinary eigenmodes. As light falls on the surface at normal incidence both ordinary and extraordinary rays will propagate in the same direction, but with different velocities. The phase change produced by propagation will then be different for the two rays. The phase change or retardation can be expressed as

$$\Gamma = \frac{2\pi}{\lambda}\left(n_e - n_o\right)d$$

Where, n_e and n_o are the extraordinary and ordinary indices, respectfully, d is the thickness.

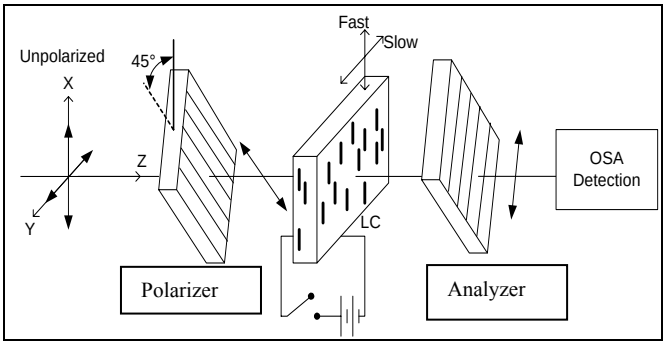

Figure 2-2. *The LC cell is shown as positioned both pre and post irradiation. The analyzer was oriented for minimum throughput transmission.*

Given the optical set-up shown in Figure 2-2, the intensity of transmittance of the system can be expressed as

$$T = \sin^2\left(\frac{\Gamma}{2}\right) \text{ (for crossed polarizers)} \quad \text{or} \quad T = \cos^2\left(\frac{\Gamma}{2}\right) \text{ (for parallel polarizers)}$$

Where, Γ is the optical retardation of the liquid crystal cell as given in the previous equation.
Then by measuring the transmission through an analyzing polarizer and matching it with the appropriate $\sin^2$ ($\cos^2$) dependence, the optical thickness or phase modulation depth can be determined. The contrast ratio is the ratio of the maximum throughput and the minimum throughput of the retarder. These measurements were made with an optical spectrum analyzer (OSA).

2.2.1 LC Cell Bias Conditions

The LC cells were tested both in unbiased and biased conditions. Biasing consisted of applying a 2 kHz, 5V pk-pk, bipolar square wave during irradiation. Biasing was removed during measurements as shown in Figure 2-2.

In keeping with MIL-STD-883, Method 1019.6, the measurements in the unbiased condition did not take more than an hour from unbiased condition of the LC to reapplying the bias.

2.3 Instrumentation

A block diagram of the instrumentation used for the retardation and contrast measurements is shown in Figure **2-3**. For these tests an optical bench was engineered which consisted of a filtered arc lamp and two linear polarizers, oriented at 45 ° and parallel with respect to each other. The LC cell was placed in between the polarizers in an unbiased condition. Optical power was measured using an Ando optical spectrum analyzer (OSA), where the throughput parameters of amplitude versus wavelength were measured. All measurements were done outside of the irradiation cell and within minutes of post irradiation exposure.

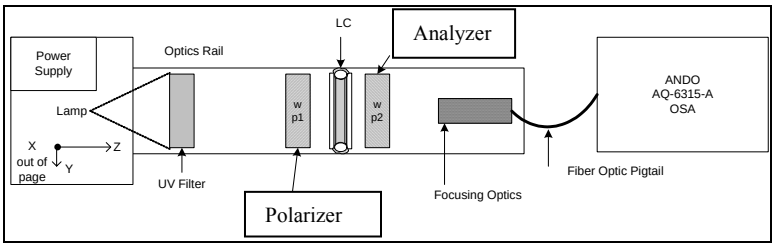

Figure 2-3. *Simplified top down view of the configuration of test equipment used to take data prior and post irradiation is shown.*

3. Part One Test Results

3.1 Test Description

The testing consisted of response analysis of twenty LC cells, ten of which were constructed with a 4.1 μm spacer for a design wavelength of 1.55 μm and the other ten constructed with a 4.9 μm spacer for a design wavelength of 2 μm. The test consisted of both thicknesses of LC cells being irradiated in the biased and unbiased condition as shown in Figure 3-1.

The parameters of interest were the null polarization of each LC cell. The null polarization was obtained by measuring the throughput by rotating one of the linear polarizers until a minimum in signal was seen at the OSA.

The LC cells were irradiated in positions determined by dosimetry to give the best uniform irradiation across the four devices. A typical configuration is shown in **Error! Reference source not found.**, where the four LC cells are positioned close to the ^{60}Co source to achieve a high irradiation dose rate.

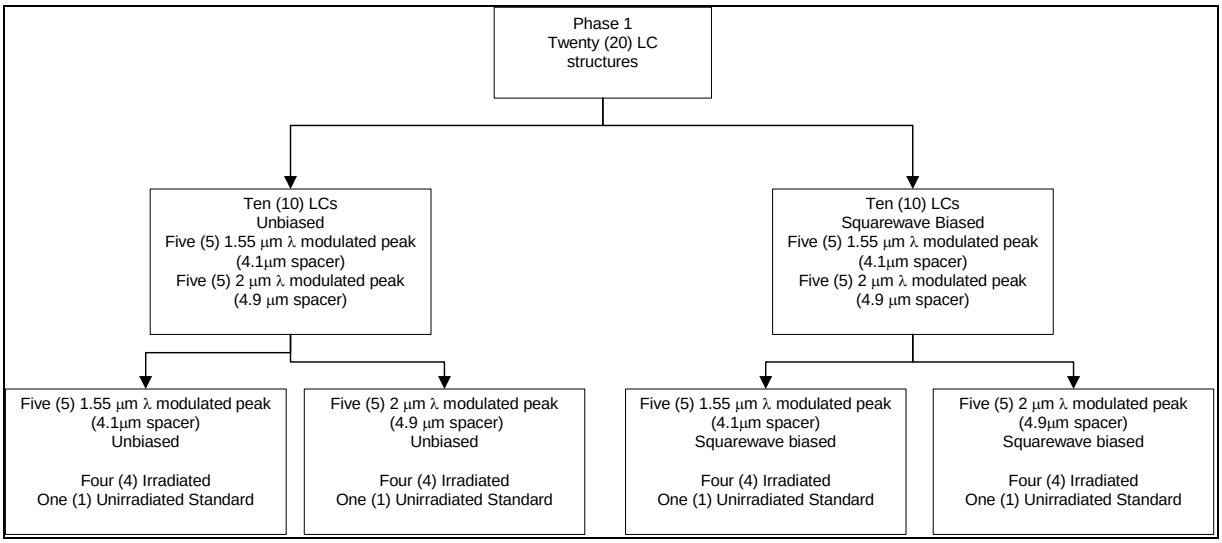

Figure 3-1. *Part One test structure of device irradiation is shown. Both types of LC devices were tested in the unbiased and biased condition.*

Specific details on each irradiation are provided in Table 3-1.

The methodology was to fully characterize each LC cell both prior to and after irradiation. This baseline characterization is shown in Test Stage 1 of the unbiased condition and Test Stage 9 of the biased condition of Table 3-1.

Table 3-1. *Part One Test Matrices Methodology for both 1.55 μm & 2 μm.*

Test Stage	Biased Condition*	Total Accumulated Dose (k rad(Si))
1	Unbiased	0
2	"	5
3	"	10
4	"	20
5	"	50
6	"	100
7	"	150
8	"	200
9	Unbiased	0
10	Biased	10
11	Biased	50
12	Biased	100
13	Biased	200

* Biased condition refers to the state during irradiation. All measurements performed with test equipment in Figure **2-3** were done in unbiased state.

Once knowledge was gained in the LC performance of Test Stages 1 through 8, the biased condition tests were accelerated in total dose deposition as indicated in Test Stages 9 through 13.

3.2 LC Response Prior and Post Irradiation

The LC pre and post irradiation response was monitored in the set-up shown in Figure **2-3** by fixing the polarizers, at 45° with respect to the LC cell and parallel with respect to each other. The LC cell is placed in the same orientation in the test set-up between each test stage in the unbiased condition. Once the LC cell is positioned the OSA is used to obtain the intensity throughput from the test set-up. All devices showed similar results to within experimental error of 1° rotation of the rotation mount.

It was seen that the unbiased LC cells of Test Stage 1 through 8 of Table 3-1 did not show degradation in the form of reduced transmission, or a decrease in contrast ratio. This was evident from the comparison of the scanned plots from the OSA to the baseline of pre irradiation for either device of 1.55 or 2 μm configuration. Since the unbiased LC cells did not show degradation the biased Test Stage increments of total dose were increased.

Data plots from the OSA are shown for a typical LC device in Figure 3-2. In Figure 3-2 both Test Stages 9 and 10 are shown from Table 3-1 for a 1.55 μm device. It is seen from the first irradiation of Figure 3-2 (middle sinusoidal graph) the peak of the transmission has moved slightly to longer wavelengths, when compared to the baseline plot, of the same figure (left sinusoidal graph). This slight shift is within measurement error. It is further seen in subsequent irradiations and plots that the peak did not move from this position with respect to increased total dose as is seen in the right sinusoidal graph of Figure 3-2. The LC devices in either the 1.55 or 2 μm configuration did not show signs of radiation induced damage.

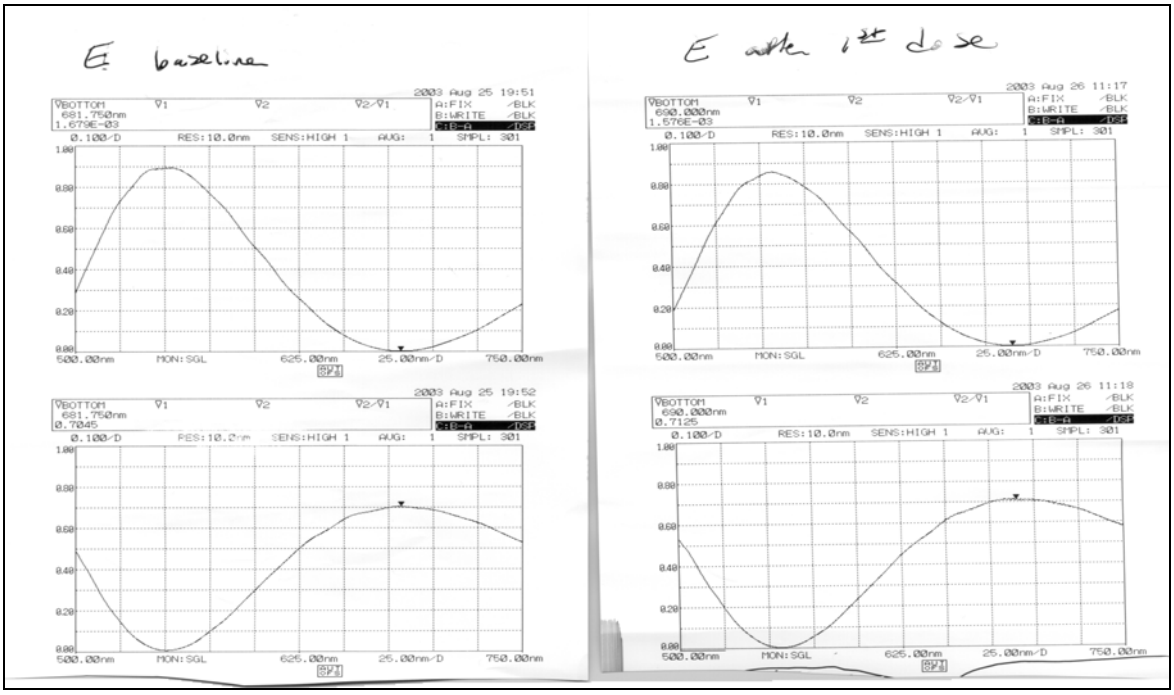

Figure 3-2. *Plots from the OSA show Test Stage 9, the Baseline (left) and the final 200k rad (right) plots from the OSA of a typical biased LC device from Table 3-1.*

Post irradiation did show degradation in the UV epoxy used to hold the bias wires against the glass cover plates, see Figure 2-1. This degradation was in the form of the UV polymer epoxy darkening, which started at a total dose of 10k rad and continued to gradually darken until saturation at 150k rad total dose. The epoxy is a u.v. curable mixture, made by Epotek, OG-142. However, the epoxy is not in the field of view of the LC material and hence had no effect on the optical operation of the devices. No further consideration was given to the darkened epoxy.

4. Part Two Test Article

Two 1x4096 SLMs were tested. The first one was tested up to a dose of 10k rad(Si) without any noticeable effects. A second device was tested up to 208k rad(Si) and the data presented below refers to this second SLM. A 1x4096 spatial light modulator is a liquid crystal cell fabricated from two dissimilar substrates one is a CMOS backplane onto which a dielectric coating has been deposited and the other substrate is ITO coated fused silica. This particular test device was gapped for a 1.55 micron wavelength. The LC cell is consistent with that described in Figure 2-1, with a few differences as shown in Figure 4-1. Most notably a cell is formed using a CMOS backplane and instead of light transmission through the SLM, light is reflected back via a mirrored interface.

4.1 Test Article Description

The CMOS backplane was made exclusively for BNS by American Microsystems Incorporated (AMI) using a 0.5 μm process. The 4096 electrodes at 1 micron thick, 7 mm long, and the pitch is 1.8 microns center to center. The SLM chip is mounted in a ceramic pin grid array (PGA). This PGA package connects to a signal conditioning board, or operational amplifier (op-amp) board via a flex circuit cable. Data of images and clocks are loaded through a computer based signal board that relays these signals through the op-amp board.

The CMOS array receives three timing signals of which a single 10M Hz square-wave timing channel clocks the transistor array. The other two timing channels consist of a 'Token Pulse' and a 'Cover Glass' clock. The Token Pulse is simply an indication to the SLM that a new image frame is being downloaded. The Token Pulse is a 100 ns wide pulse, which corresponds to the time it takes to download an image frame onto the SLM every 25.6 μs. The Cover Glass clock is a 1.5k Hz square wave clock that is normally (Type A operation - to be discussed below) operated 180 degrees out of phase with the data lines. This effectively doubles the electric field experienced by the LC and also keeps the liquid crystal DC balanced. In addition, to the three timing clocks the array has 16 data channels used to input analog image data and the primary analog bias of 5V to the array. All channels to the SLM CMOS array are inputs. All inputs to the array pass through an operation amplifier (op-amp) board to amplify the signals and provide impedance matching to a level acceptable to the SLM.

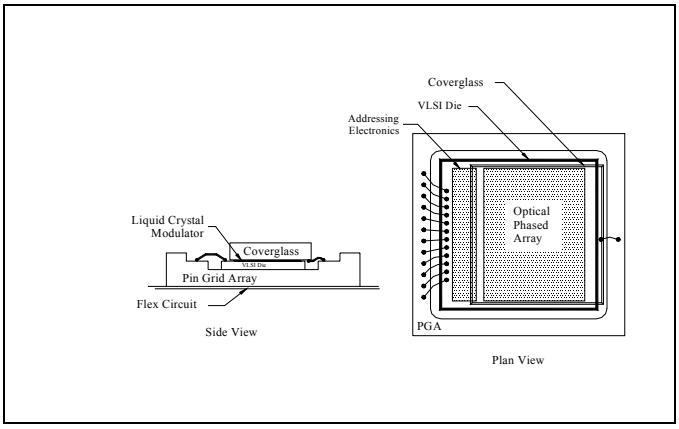

Figure 4-1. *Generic Reflective SLM is shown with the CMOS backplane. The liquid crystal is bounded by a fused silica optical flat, coated with a conductive ITO material, and the CMOS back plane. Side View and Plane View show the BNS SLM layout in detail.*

4.2 Operational Parameters

In Part One it was noted that the LC did not show degradation within experimental limits of the measurement.

Hence, the assumption going into Part Two testing was that if irradiation degradation occurs within the SLM, it will most likely occur within the CMOS backplane of the SLM.

Due to the Compton effect, ionizing (high energy gamma) radiation will produce electron-hole pairs in oxides in the CMOS backplane of the SLM. Electron-hole pair production is the predominate total dose effect in CMOS. Of these electron-hole pairs a fraction will become trapped in the oxide and a fraction cause the release of hydrogen which will induce interface electron-hole traps at the Si/SiO2 interface. In addition to oxide-trapped charge and buildup in gate oxides of interface trapped charge, ionizing radiation induced charge will also buildup in field oxides and silicon-on-insulator (SOI) buried oxides. Degradation of circuits to the point of circuit failure can be caused by the charge buildup in field and buried oxides.

As shown in Figure 4-2, when Vg goes to 0V this will cause an increase in current in the primary bias power supply. According to the literature, in ICs with very thin gate oxides the predominate radiation induced degradation is charge buildup in field oxides and buried SOI oxides.

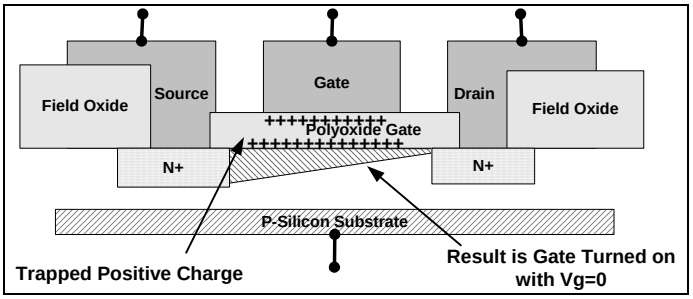

Figure 4-2. *The primary cause of circuit degradation due to ionizing radiation is buildup of charge in oxide layers. Here charge buildup in the gate oxide results in leakage current in the OFF state of Vg=0V. This causes an increase in the current of the primary bias power supply.*

Two parameters were measured during the testing of the SLM, which were CMOS current and qualitative modulation depth. The relation of retardation and modulation depth were discussed in Section 2.2 above. The primary CMOS current was measured at the op-amp board, which supplies all clocks, data channels and bias signals to the SLM. The CMOS biasing voltage, or current draw is a direct indication of the CMOS back plane electronic operational functionality. The CMOS current was measured at a signal junction on the op-amp board.

The modulation depth is related to retardation and was monitored qualitatively by visual observation via a microscope and digital camera. The images obtained through the microscope and digital camera, show the refractive patterns and are an indication of the modulation depth of the SLM. These refractive patterns are similar to the sinusoidal plots (see Figure 3-2) obtained in Part One for the LC cells from the OSA. Images of the SLM were obtained for four different patterns. The two parameters where measured while under biased conditions during all pre and post irradiations.

4.2.1 Instrumentation

Instrumentation for Part Two experiments consisted of that shown in Figure 4-3. The SLM patterns were initiated at the computer through a program and originate at an interface board with a 16 bit data port. These signals are then amplified to levels acceptable to the SLM through an operational amplifier board.

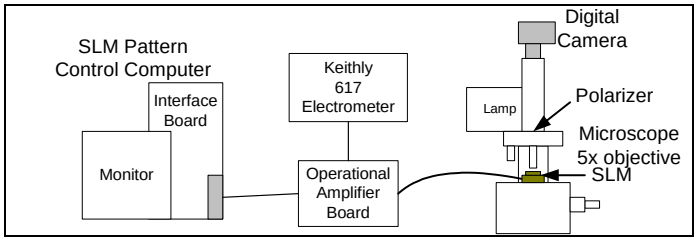

Figure 4-3. *A simplified schematic of the equipment set-up to monitor the SLM is shown.*

The CMOS current was monitored at the operational amplifier board through the primary transistor bias signal. An electrometer was inserted in series into the primary SLM bias signal path. In order not to disrupt the pictures taken to gauge modulation depth, the electrometer was taken out of the equipment set-up and jumpers used for continuity on the op-amp board of the primary bias signal.

4.2.2 Data Analysis

The measurement of the width of the refracted light on the imaged patterns is directly proportional to the optical thickness of the LC material. Since the SLM is crossed between a polarizer within an imaging microscope the imaged patterns show a spatially varying retarder. These patterns are analogous to the transmission variation of the Part One scans obtained with the OSA. These sinusoidally varying patterns are evident in the colored bands of decreasing thickness. The colored bands seen in the images correspond to the wavelengths that are passed. Since the SLM is acting like a retarder the transmission will be proportional to $\sin^2 \Gamma$.

The CMOS current was measured as a function of total absorbed dose and time of anneal. Increase in primary current power is a well known effect of radiation on VLSI circuits. The current increase is explained by the charge buildup in oxide layers within the CMOS structure. Hence, at the onset of the experiment, it was believed the SLM will gradually degrade until failure with increased total dose as a function of CMOS current increase.

4.3 Part Two Test Results

4.3.1 Test Description

As discussed above, the first SLM, serial number BS145, was irradiated to a total dose of 10 k rad(Si) without effect. Due to scheduling conflicts, further irradiation of BS145 would not have conformed to MIL STD 883. Consequently, a second irradiation test was performed on a different SLM. The second SLM, serial number BS223, was irradiated according to
Table 4-1. Irradiation occurred without delays other than the time to measure the parameters of interest. The measurements were made within one hour from the stop of irradiation and the irradiation continued within two hours from stop to the start of the next Test Stage.

Due to the limiting length of the flex circuit, which connects the SLM to the op-amp board, the SLM was placed farther away from the ^{60}Co source than the LC cells in Part One testing. This resulted in a dose rate of 1.5 rad/sec. Hence, this would mean this testing was not a Condition A in MIL STD 883 Part 1019 of 50 to 300 rad/sec, but instead would conform to Conditions B and C of the MIL STD 883.

While being irradiated the SLM was powered with a separate op-amp board in the irradiation cell. Each time the SLM was powered on before irradiation, the image patterns loaded into the SLM were checked visually to confirm the SLM was properly functional. Then after each irradiation and prior to powering down the SLM, the same procedure was used to confirm no latch-up occurred during irradiation.

Table 4-1. *Part Two Test Methodology.*

Test Stage	Total Dose rad(Si)	Time to Total Dose (hrs)
1	0	0.0
2	1000	0.2
3	2000	0.2
4	5000	0.5
5	10000	0.9
6	15785	1.0
7	20000	0.8
8	30000	1.8
9	50000	3.6
10	110991	11.0
11	174755	11.5
12	208577	6.1
Total	**208577**	**37.6**

Test Stage	Post Anneal Time from Test Stage 12 (hrs)
13	44
14	72
15	100
16	118
17	402

After the end of irradiations at Test Stage 12 of Table 4-1, the SLM was held in a continuous biased state and allowed to anneal at room temperatures. Over the course of 16 days the device was observed and data recorded.

4.3.2 *Modulation Depth Data Photographs*

A direct indication of the functionality of the SLM, albeit qualitative, is an image of the SLM. Images of the SLM were taken in all Test Stages shown in

Table 4-1. Images were taken for all four image patterns. The four image patterns vary the voltage across the cover glass in a saw-tooth manner. The LC material responds with respect to the varying voltage across the LC cover glass and hence the retardation is varied accordingly. This variation is seen as a repeating rainbow pattern across the LC in visible light. Visible light is being refracted through the LC material and reflected back from the mirror, which acts as a boundary layer for the LC material.

The four different patterns introduced into the SLM were to examine the different modes of the SLM. Of the four different image patterns the pattern with the most structure is referenced in this report. Table 4-2 shows a general description of the four image patterns.

Of the four image patterns, the greatest modulation depth structure and hence the most interesting is that of image pattern 3. Consequently, pattern 3 photos are referenced in this report.

Table 4-2. *SLM image pattern nomenclature.*

Modulation Pattern	Nomenclature of Structure
0	Device Half On
1	Reverse of Pattern 0
2	Structured Modulation
3	Greatest Structured Modulation

Shown in Figure 4-4 is a layout of the SLM as it would appear to an incoming optical wave.

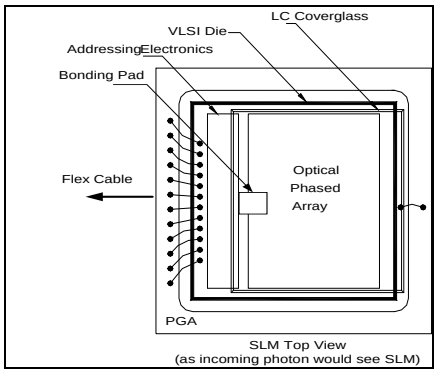

Figure 4-4. *A close-up of the SLM is shown. Note the bonding pad. This bonding pad was used in all photos as a key feature landmark.*

In addition to the four image patterns of Table 4-2, two variations of those images were examined. These two variations, or types correspond to the two types of clocked voltages used for the Cover Glass signal. Type A results in the SLM being operated with a variable amplitude AC signal.

Type A operation is normal or typical operation. Type B resulted in the SLM being operated in a DC biased mode Type B is not a typical operation mode for an SLM. The differences are easily visually noticed in the photo images themselves in that Type A operation is seen with more vivid colors hence better efficiency in modulation depth and Type B with dulled colors or less efficiency in modulation depth.

The differences in Type A and Type B operation are in the Cover Glass clock signal, which is terminated on the fused silica cover glass. The Cover Glass clock supplies the bias voltage via the ITO electrode on the LC cover glass. When the voltage applied to a given pixel within the CMOS is greater, or less than the Cover Glass voltage, the pixel is said to be in a driven state. When the voltage applied to a given pixel within the CMOS matches the voltage on the Cover Glass the LC at that pixel is in an 'off' state, which is un-switched, or is said to be un-driven. In this un-driven state, the LC returns to a relaxed state. This type of switching describes Type A operation. However, Type B operation is in a quasi-on state, in that the liquid crystal in the SLM is biased and operating around a partially switched state.

A marked contrast is seen in Type A and Type B operation in Figure 4-5, where both Cover Glass clocked voltages as fed into the SLM are shown. It is apparent that Type B operation is extremely long in time base cycle compared to that of Type A operation. Thus for Type B operation, the Cover Glass signal can not be 180 degrees out of phase with the signals on the data lines and the SLM is not DC balanced. Also apparent in Type B operation is the noise in the voltage level.

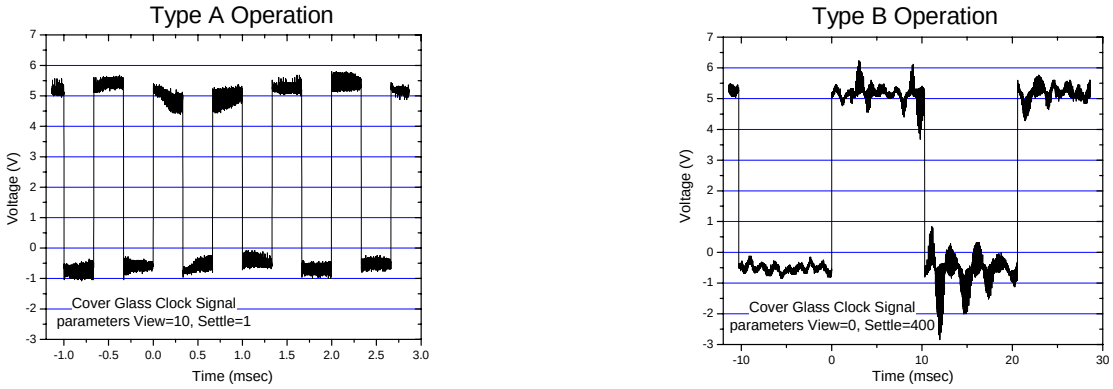

Figure 4-5. *The Cover Glass signal as input into the SLM is shown in two different cases. Type A operation is representative of typical liquid crystal driving. Type B operation is representative of a quasi--driven state.*

No visible degradation was seen in the images of any of the addressing patterns for type A operation. Images of pattern 3 are shown in Figure 4-7, corresponding to a few of the test stages of
Table 4-1. What was measured here is the width of the first order blue band. It is seen that the width of this band does not change through irradiation. Hence, the result can be inferred that the modulation depth at zero incidence angle was unaffected by irradiation. It is seen in Figure 4-7 that the appearance of the image is somewhat out of focus. This is due to an error in adjustment of focus in the microscope. The focus error was corrected and is seen in Figure 4-7 on the right. The measurement of width of the first order blue band on the photos is seen to be unaffected by the initial defocus of the image during the test.

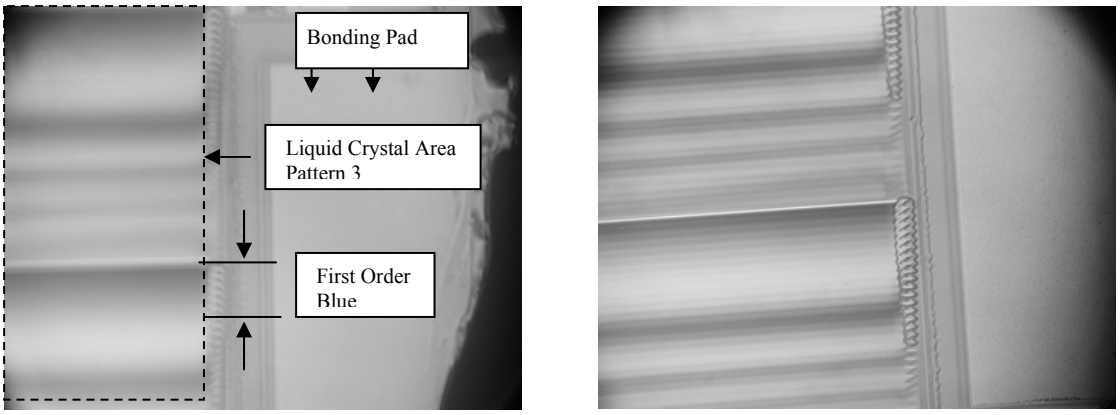

Figure 4-6. *Type A operation, Pattern 3. Left is the Baseline. Right is the 208k rad(Si) total dose irradiation. Note the yellowed appearance is due to the microscope lamp and not an effect of irradiation.*

Any rotation in the photos is due to the camera mount rotation on the microscope and not the microscope polarizer with respect to the SLM. Type A operation showed no indication of degradation due to irradiation in any of the four modulation patterns. Comparisons of the first order blue show no sign of reduction in width of the band.

However, Type B operation did show degradation that occurred with increasing radiation dose in the form of the disappearance of the first order red line. Type B operation is not typical of liquid crystal device operation. As discussed above, for Type B operation, the device is DC biased and operating in a partially switched mode and not conducive to normal operation. Degradation can be seen for Type B operation in the sample photos, all taken within minutes after irradiation. It is clearly evident that the first order red line is receding with increasing total dose. This

observable degradation is first evident at a total dose of 15.7k rad(Si). The first order red line is completely absent at Test Stage 9 of total dose 50k rad(Si).

This apparent degradation in the line width of modulation can be correlated to a degradation of modulation depth of the SLM and hence the performance of the device. However, it is worth remembering here that the SLM in Type B operation is not driving the liquid crystal material as it would normally be driven. The question then becomes why does Type B differ from Type A in terms of susceptibility to total dose irradiation? A hypothesis proposed here is that the DC bias present in Type B operation causes space charge build-up that is further acerbated by the presence of ionizing radiation. This hypothesis was not further examined in this Phase I study.

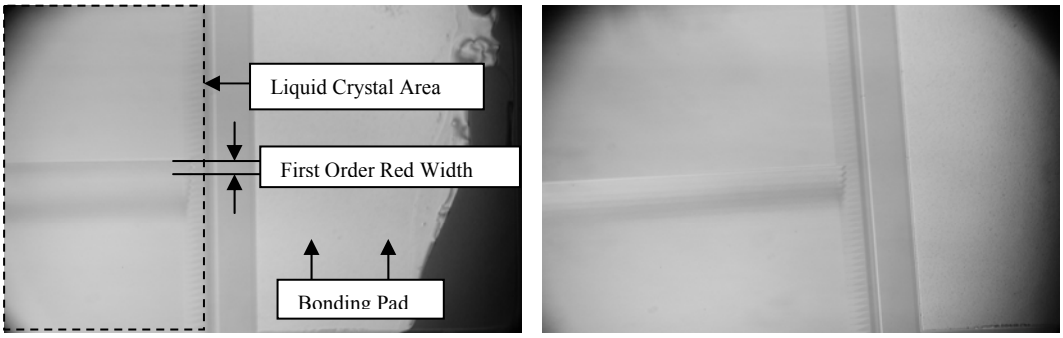

Figure 4-7. *Type B operation, Pattern 3. Left is the Baseline. Right is the 208k rad(Si) total dose irradiation. Note the yellowed appearance is due to the microscope lamp and not an effect of irradiation.*

After irradiation the SLM was held in the biased condition at room temperatures for a period of about 16 days with the same four patterns being introduced to the SLM. During this anneal time the same data was taken as during irradiation. As anneal time increased Type B operation showed the first order red line width recovering. After 402 hours of anneal time the first order red clearly re-emerged.

4.3.3 CMOS Current

Current increase due to irradiation induced charge build up, is a well documented effect of gamma radiation on CMOS devices and was seen to increase with dosing the BNS OPA. The current baseline prior to irradiation was seen to be about 7.8 mA. Since this current was in the mA range this mitigated the associated troubles with any triboelectric effect error in moving of cables in between the Test Stage sequences. Triboelectric effects were present and on the order of μA range, adding to the variance in measurements, but of a minor concern, given the mA range amplitude of the signal.

All four patterns introduced to the SLM had similar CMOS input current responses and varied between patterns in the tenths of mA. A threshold of observable current increase started at 15.7 krad(Si) (shown in Figure 4-11), which is the same threshold for Type B operation of the SLM corresponding to the first order red degradation.

Figure 4-, and Figure 4-8 demonstrate, that the current first increases to a peak of 19.1 mA at 111k rad(Si), then with increasing dose drops to 17.9 mA at 208k rad(Si). The current increase in the CMOS was discussed in Section 4.2 and is likely due to the trapped charge buildup in oxide layers. However, this does not explain the decrease in current with increased absorbed dose. It is hypothesized here that another damage mechanism is dominating within the CMOS, which limits its current draw. It is possible that a new current leakage path within the CMOS was formed and is allowing charge buildup to migrate out of the oxide layers. Further investigation of this damage mechanism is warranted, but was not in the scope of this initial investigation.

Six sigma variance in current measurements showed about a 2% deviation from the measured values and hence were not plotted in

Figure 4-, and Figure 4-8.

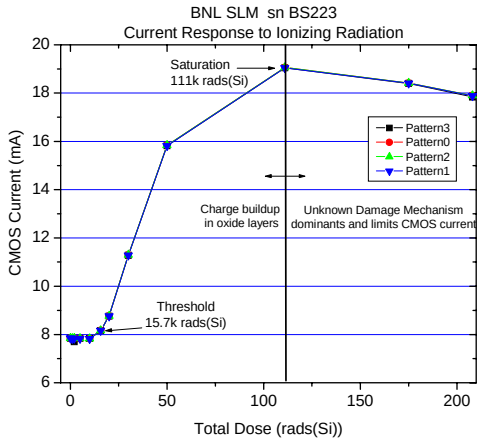

Figure 4-10. *Current response of the primary CMOS power supply for the SLM is shown. Threshold response appeared at 15.7 krad(Si). Saturation of the power supply current appeared at 111k rad(Si). Beyond 111k rad(Si) an unknown damage mechanism within the CMOS limits the current increase. The unknown damage mechanism is most likely a new leakage path dominating the degradation.*

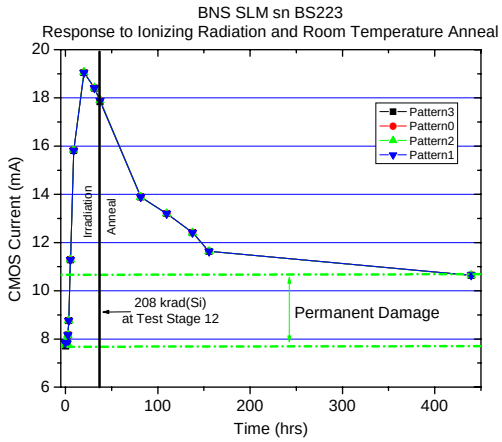

Figure 4-8. *During irradiation it is seen the current increased to a peak of 19.1 mA from a nominal value of 7.8 mA. After some 402 hours of anneal at room temperature a permanent CMOS current increase of 2.9 mA is seen.*

Despite the correlation of increasing current to Type B operation degradation of the first order red, no apparent degradation was seen in Type A operation, which is more representative of normal operation within a beam deflector application. In both operation types of A and B, the measurement error is the resolution of measurement in the width of the imaged photo modulation.

5. Conclusions

The Part One test, in which liquid crystal cells were evaluated demonstrated that the material appears immune to total ionizing dose up to 200k rad(Si) with respect to retardation and contrast ratio. All parameters measured on all LC devices were within error bar limits of measurement.

It is possible that the lack of degradation with irradiation for the LC is because of the material structure of the LC itself. However, one should note that given the darkening of the Epotek polymer epoxy suggests that polymer dispersed or polymer stabilized liquid crystal modulators might be susceptible to irradiation damage.

The Part Two testing in which the SLM device was evaluated did demonstrate an increase in the CMOS primary power bias current from 7.8 mA to a peak of 19.1 mA for a total dose of 111k rad(Si). Above 111 krad(Si), as is apparent in the data another damage mechanism starts to dominate over the charge buildup in oxide layers.

In Part Two tests the SLM was driven in two different modes, Type A operation, which is representative of a real-world application, showed no apparent degradation due to irradiation to within the qualitative measurement methods used. Type B operation, which has a DC component and is not a normal operational mode, did show degradation with increasing total radiation dose. The hypothesis proposed here is that in Type B operation, the DC bias present caused charge build-up that is further acerbated by the presence of ionizing radiation.